Plasma-Assisted Cleaning by Metastable-Atom Neutralization (PACMAN): A Plasma Approach to Cleanliness in Lithography

W.M. Lytle[a], D. Andruczyk[a], V. Jindal[b], and D.N. Ruzic[a]

[a]**Center for Plasma-Material Interactions, University of Illinois at Urbana-Champaign**
[b]**Sematech**

Abstract. The Plasma-Assisted Cleaning by Metastable-Atom Neutralization (PACMAN) cleaning technique being developed in the Center for Plasma-Material Interactions (CPMI) at the University of Illinois at Urbana-Champaign is a dry-non-contact vacuum-based removal technique. The PACMAN process uses a high density helium plasma (ne $\approx 10^{17}\mathrm{m}^{-3}$, Te $\approx$ 3eV) to achieve removal of organic contaminants on optical masks, EUV masks, silicon wafers, and optics material used in integrated circuit manufacturing. The PACMAN process is successful at removing both hydrocarbon particles as well as carbon layers by utilizing the high-energy helium metastables in the plasma. The helium metastables, with 20eV of energy, are used to break the bonds of the particle allowing for volatilization or desorption of the atoms/hydrocarbon chains of the particle to achieve an etching-like removal method without using traditional etchant process gasses. With ion energies of 10eV, damage such as surface roughening or surface erosion to the underlying structures being cleaned are avoided. Also, film densification (the removal of hydrogen from a hydrocarbon resulting in a dense carbon layer at the surface of the particle) is avoided in the PACMAN technique due to the absence of high-energy ions which would preferentially sputter hydrogen out of the particle matrix. Preliminary results for the removal of polystyrene latex nanoparticles in the range of 30 nm to 500 nm have shown removal rates of 1.2x10^7 $\pm$ 5.1x10^5 nm^3/min without damage to silicon wafers. Also, carbon films on silicon wafers have been removed with the PACMAN technique at a rate of 3.0x10^6 $\pm$ 1.3x10^5 nm^3/min. Current results of cleaning various particle types from surfaces through the PACMAN process will be presented in addition to a theoretical model of the removal process.

Send correspondence to David Ruzic
E-mail: druzic@illinois.edu, Telephone: 1-217-333-0332

Extreme Ultraviolet (EUV) Lithography II, edited by Bruno M. La Fontaine, Patrick P. Naulleau, Proc. of SPIE Vol. 7969, 796927 · © 2011 SPIE · CCC code: 0277-786X/11/$18 · doi: 10.1117/12.881038

1 INTRODUCTION

A challenge in any lithography system is cleanlines since defects that result in pattern-transfer errors from the lithographic mask to the wafer to be patterned will reduce throughput, decrease the chip's reliability and lifetime, and decrease profits for the chip maker. The extension of traditional wet-cleaning techniques to extreme ultraviolet lithography (EUVL) photomasks is limited due to small size of the contaminants being cleaned since wet-cleaning techniques rely on momentum-transfer to the particle in order to achieve removal. Also, the chemicals the comprise the cleaning solutions can have an etchant effect on the photomask surface that has the potential to lead to feature devolution (insert citation). An additional challenge is seen when considering EUV photomasks compared to optical lithographic masks. A pellicle (a thin transparent membrane to protect the photomask) is transmissive to the 193 nm light used in optical lithoraphy, however, a pellicle that is transmissive to EUV light at 13.5 nm for use with EUVL systems is not currently available.

In addition to contamination of the photomask during use, problems arise during the fabrication of a photomask that can effect the reflective nature of the EUV light. A particle that is on the surface during multilayer deposition during EUV photomask fabrication can yield errors in the underlying structure of the mask.

When considering a cleaning technique that can be applicable to a manufacturing environment, the technique should be quick, non-damaging, not introduce more contaminants to the surface being cleaned, and compatible with the current process flow of chip production. Other cleaning techniques such as laser-shockwave cleaning and CO_2 snow cleaning are potentially useful, however the risk of damage from the shockwave and the issue of the speed in rastering a CO_2 beam across a surface to be cleaned are problems that still need to be addressed and refined.

A new cleaning technique that is quick, non-damaging, non-contaminating, and compatible with the current process flow of chip production is being developed at the Center For Plasma-Material Interactions at the University of Illinois Urbana-Champaign (UIUC). This process, the Plasma-Assisted Cleaning by Metastable-Atom Neutralization (PACMAN) technique, is a plasma-based cleaning technique that utilizes metastable atoms from the plasma in order to clean surfaces. The following sections outlines the theory behind the cleaning technique as well as the results of the removal of hydrocarbon contaminants from silicon wafers (representing lithographic material).

The PACMAN cleaning technique is carried out in the Plasma-Assisted Cleaning Experiment (PACE) chamber in the Center for Plasma-Material Interactions (CPMI) at UIUC. The chamber consists of a loadlock chamber, processing chamber, m=0 helicon plasma source with auto-matching network, and class 100 laminar flow clean hood. The m=0 helicon plasma source produces plasma of approximately 3 eV and densities on the order of 10^{16} m^{-3}. A diagram and picture of the PACE chamber can be seen in Figure 1.

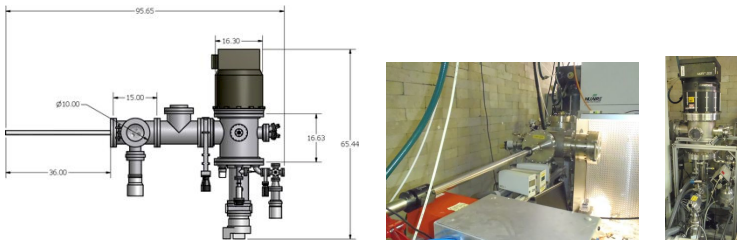

(a) (b) (c)

Fig. 1. A computer aided drawing and pictures of the PACE chamber in the Center for Plasma Material Interactions at the University of Illinois Urbana Champaign. The PACE system consists of two chambers, a sample transfer chamber, and a main chamber. All dimensions are in inches.

2 THEORY AND MODELING

When a plasma is formed, energetic ions and electrons are created in the plasma and are typically what are important to the engineer creating the plasma. However, there is a strong energetic neutral component in plasmas too in the form of metastable atoms. Metastable atoms are those that are stuck in a quantum state and are forbidden through conservation of momentum from decaying to the ground state (such as 2s to 1s transitions being forbidden). Thus, any electron entering the 2s state will be hypothetically 'stuck.' In general, the lifetime of these metastable atoms is low, so they don't often play a significant role. There are two metastable states in helium, singlet 2s and triplet 2s, with 20.616 eV and 19.820 eV of energy each as seen in Figure 2 with lifetimes on the order of seconds [1, 2]. Helium plasma has been used for the current work due to its low sputtering threshold on lithographic material (due to its low mass), in order to achieve particle removal.

The three parameters of the plasma that have been identified as important to the removal mechanism are the density of helium metastable atoms in the plasma and thus there flux to the surface, the electric field in the plasma sheath, and the flux of electrons to the sample being cleaned. The helium metastables play the role of introducing electronic 'holes' in the surface by breaking bonds, the electric field maintains broken bonds at the surface of the particle, and electron flux to the surface keeps broken bonds from reforming. Each of these parameters is discussed in further detail in the following sections.

2.1 Helium Metastable Interaction With Surfaces

Metastable atoms and their interaction with surfaces have been studied for several different purposes: metastable probes, metastable beam lithography, and their role in desorbing gas species from surfaces [3–5]. There are two primary interactions that can occur when a metastable interacts with a surface; resonance ionization (RI) followed by Auger neutralization (AN) on a conductor or Penning ionization (PI) which is also known as Auger de-excitation (AD) on an insulator. When a metastable atom collides with an ordinary metal, the 2s electron of the helium metastable tunnels into an empty level in the surface of the metal forming a helium ion. This process is called resonance ionization. This helium ion is then neutralized by an electron from the surface followed simultaneously by the emission of another surface electron. This process is called Auger neutralization [6]. However, on an insulator, resonance ionization is suppressed because the 2s level of the helium metastable falls within the energy gap of the insulator. Thus, as the helium metastable interacts with the surface, an electron from an occupied orbital from the surface will transfer to the helium metastable with the subsequent ejection of the 2s electron [6].

In a study by Kurahashi et. al [7]. examining desorbtion of hydrogen from a surface, they conclude that if the helium metastable extracts a bonding electron from the hydrogen-surface bond, the bond becomes weaker. As the bond becomes weaker, the equilibrium bond distance lengthens. This weakening and lengthening of the bond changes the potential of the hydrogen-surface bond and the hydrogen can desorb from

the surface [7]. A similar method is theorized to be the cause for the helium metastable cleaning of organic material.

2.2 Helium Metastable Modeling

The density of helium metastable atoms in the plasma can be modeled through a collisional-radiative model. In this type of model, it is possible to track the population and decay of higher energy levels of the helium atom that would result in a metastable atom in the 2s singlet or triplet level. The number of higher energy states to track depends on the complexity necessary to capture the major collisional and radiative processes. The extent to which the higher energy levels will be used to determine population states of the lower energy levels needs to be limited to some finite value based on the probability of the reactions. For this CR model, states up to and including the 3s and 3d state are used to calculate the population of the excited levels in the helium plasma. A graphical view of the balance of the helium metastable singlet state is seen in Figure 3. The boxes on the left represent the states that have a transition into the singlet metastable state, while the boxes on the right represent the states that the singlet metastable state transitions into. Boxes connected to the central term (that being balanced) with an arrow is an electron-collision process with the corresponding reaction rate k listed on the left. The subscript label on the 'k' term is representative of the initial state and final state and corresponds to the reaction rate for that transition. The boxes not connected by arrows are the radiative transition terms. For the singlet metastable state, the mathematical balance of equations is:

$$k_{02}n_e n_i + k_{12}n_1 n_e + k_{32}n_e n_3 + N_{21p}(0.01976x10^8) + N_{31p}(0.1338x10^8) \\ -n_2(\phi_2 + n_e(k_{23} + k_{21s31p} + k_{21s23p} + k_{21s0})) = 0, \quad (1)$$

Similar equations can be written for the other states in the plasma, as shown below.

$$k_{03}n_e n_i + k_{23}n_e n_2 + k_{13}n_e n_1 + N_{23p}(0.1022x10^8) + N_{33p}(0.09478x10^8) \\ -n_3(\phi_3 + n_e(k_{32} + k_{23s21p} + k_{23s23p} + k_{23s33p} + k_{23s0})) = 0, \quad (2)$$

$$k_{11s21p}n_e n_1 + k_{23s21p}n_e N_3 + k_{21s21p}N_2 n_c + k_{23p21p}N_{23p}n_e + N_{31d}(0.638x10^8) \\ +N_{31s}(0.181x10^8) - N_{21p}n_e k_{21p31d} - N_{21p}n_e k_{21p0} \\ -N_{21p}(17.99x10^8) - N_{21p}(.01976x10^8) = 0, \quad (3)$$

$$k_{21p31d}n_e N_{21p} + k_{11s31d}n_e N_1 - N_{31d}(0.638x10^8) = 0, \quad (4)$$

$$k_{11s33s}n_e n_1 - N_{33s}(0.278x10^8) = 0, \quad (5)$$

$$k_{11s33p}n_e n_1 + k_{23s33p}N_3 n_e - N_{33p}(0.09478x10^8) = 0, \quad (6)$$

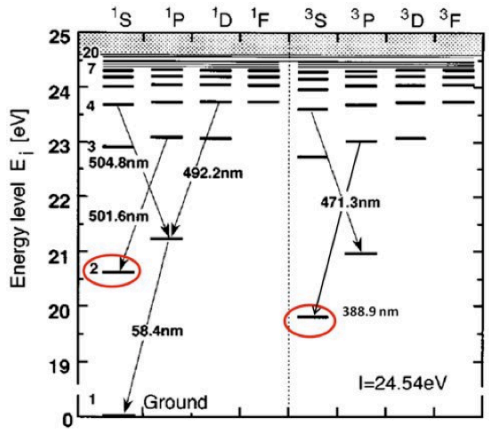

Fig. 2. A diagram of the energy levels of the helium atom. The two circled levels represent the metastable energy levels which are quantum mechanically forbidden from decaying to the ground state energy due to the conservation of angular momentum. Diagram from Sasaki et. al. [1]

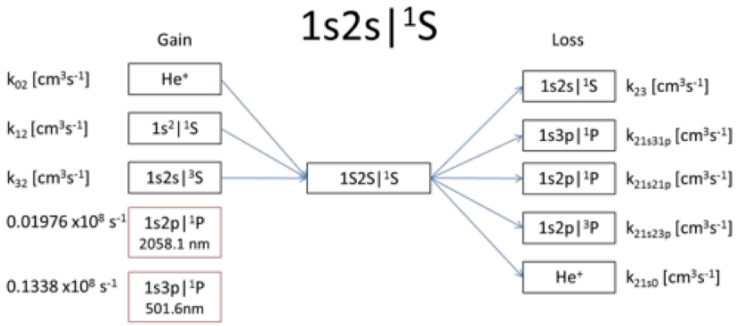

Fig. 3. A graphical representation of the transitions into and out of the singlet metastable state. Boxes connected to the central term being balanced connected with an arrow are electron-collision processes whereas the boxes not connected by an arrow are radiative transitions.

$$k_{11s31p}n_e n_1 + k_{21s31p}n_e N_2 - N_{31p}(5.66x10^8) - (0.1338x10^8)N_{31p} = 0, \quad (7)$$

$$k_{23p33d}n_e N_{23p} - N_{33d}(0.706x10^8) = 0, \text{and} \quad (8)$$

$$k_{11s31s}n_e n_1 - N_{31s}(0.181x10^8) = 0. \quad (9)$$

The resulting metastable densities in Figure 4 and Figure 5 show an increasing trend in density as electron temperature increases as well as operating pressure increases. At slightly greater than 100 mTorr, a decrease in the population of the metastable states

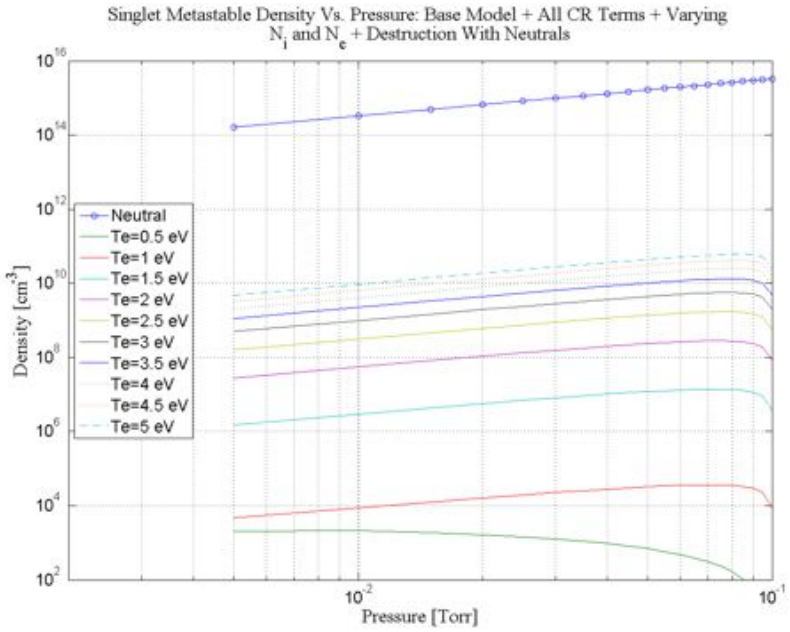

Fig. 4. Shown is the singlet metastable density versus pressure accounting for transitions into the metastable state from higher energy levels as well as allowing for ion, electron, and pressure variations.

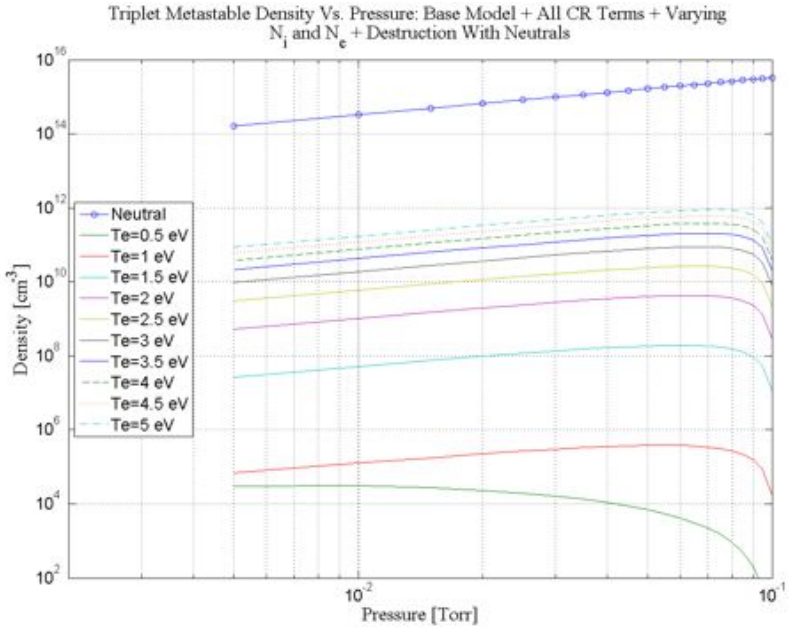

Fig. 5. Shown is the triplet metastable density versus pressure accounting for transitions into the metastable state from higher energy levels as well as allowing for ion, electron, and pressure variations.

is predicted indicating a transition between a plasma dominated by metastable loss to the wall to destruction from neutral collisions as well as less metastable production due to increasing electron-neutral collisions. The theoretical results rely heavily on assumptions made for electron density and temperatures as no Langmuir probe data was acquired in this pressure range. Thus, the graphs have been truncated at 100 mTorr as measured data and thus accuracy for the theoretical predictions in this pressure range are more reliable.

This model, while it calculates the singlet and triplet metastable densities, is only accurate for the specific input parameters, namely operating pressure, electron density, ion density, and electron temperature. Thus, reliable measurements of the input parameters will yield more accurate results.

2.3 Electric Field In The Plasma Sheath

In order to calculate the electric field in the plasma sheath, one starts from Poisson's equation with three assumptions. The first assumption is that electron density in the sheath is zero, $n_e = 0$. The second assumption is that the ion density, n_i, varies in the sheath from the potential variation, and that the energy of ions are zero at the plasma/sheath boundary, x=0. One begins by writing Poisson's equation [8]:

$$\nabla^2 V = \frac{-\rho}{\epsilon_0}. \tag{10}$$

Then,

$$\nabla^2 V = -\frac{e n_i}{\epsilon_0}, \tag{11}$$

applying the assumption that n_e =0 in the plasma sheath. 'e' here is introduced as elementary charge. Ion density variation in the plasma sheath varies according to [9]:

$$n_i(x) = \frac{J_{i,0}}{e}\left(-\frac{2e\cdot V}{m_i}\right)^{-1/2}, \tag{12}$$

where $J_{i,0}$ is the constant ion current and m_i is the ion mass. In one dimension, the above equation reduces to:

$$\frac{d^2V}{dx^2} = -\frac{J_{i,0}}{\epsilon_0}\left(-\frac{2e\cdot V}{m_i}\right)^{-1/2}. \tag{13}$$

Multiplying both sides by $\frac{dV}{dx}$, on obtains:

$$\frac{dV}{dx}\left(\frac{d}{dx}\left(\frac{dV}{dx}\right)\right) = \frac{dV}{dx}\frac{a}{\sqrt{V}}, \tag{14}$$

where

$$a = -\frac{J_{i,0}}{\epsilon_0}\sqrt{\frac{m_i}{2e}}. \tag{15}$$

It is convenient now to note that:

$$\frac{d}{dx}\left(\frac{dV}{dx}\right)^2 = 2\frac{dV}{dx}\left(\frac{d}{dx}\left(\frac{dV}{dx}\right)\right), \tag{16}$$

and

$$\frac{d}{dx}\left(a\sqrt{V}\right) = \frac{a}{2\sqrt{V}}\frac{dV}{dx}. \tag{17}$$

Applying the above two substitutions to equation 14 and integrating both sides, one obtains:

$$\int_0^x \frac{d}{dx}\left(\frac{dV}{dx}\right)^2 = \int_0^x 4\frac{d}{dx}\left(a\sqrt{V}\right). \tag{18}$$

Integrating the above equation and utilizing that ion energy is zero at the sheath boundary, one obtains:

$$\left(\frac{dV}{dx}\right)^2 = \frac{4J_{i,0}}{\epsilon_0}\sqrt{\frac{m_i}{2e}}\sqrt{V}. \tag{19}$$

Taking the square root of each side, one obtains:

$$\frac{dV}{dx} = 2\left(\frac{J_{i,0}}{\epsilon_0}\right)^{1/2}\left(\frac{2e}{m_i}\right)^{-1/4}(|V|)^{1/4}\cdot \text{sign}(V). \tag{20}$$

One could continue on to calculate the potential versus location in the plasma sheath, however, knowing that $E = -\frac{dV}{dx}$, the electric field in the plasma sheath has been derived without making the assumption that V_{plasma} - V_{wall} is $\ll T_e$. The electric field in the plasma sheath region is thus:

$$E = -2\left(\frac{J_{i,0}}{\epsilon_0}\right)^{1/2}\left(\frac{2e}{m_i}\right)^{-1/4}(|V|)^{1/4}\cdot \text{sign}(V). \tag{21}$$

One note of clarity in equation 21 is needed. The value of potential, V, used in equation 21 has absolute value signs around it due to the raising of V to the 1/4 power. The value of potential, V, used is the potential with respect to plasma potential, which is found by $V_{wall,bias}$ - V_{plasma}. The term sign(V) is used to denote the direction of the electric field. When the electric field points from the plasma into the surface (when V in equation 21 is negative), this is considered a positive electric field. When the electric field points from the surface into the plasma (when V in equation 21 is positive), this is considered a negative electric field.

One conclusion apparent from the result derived in equation 21 is that the electric field does not depend on the location within the sheath. Thus, the electric field is considered constant throughout the plasma sheath.

2.4 Electron Flux

Electron flux to the surface is dependent on the densities of electrons in the plasma as well as the velocity of the electrons. Assuming a Maxwellian energy distribution for the electrons in the PACE helicon plasma source, the flux of electrons to the surface is given as [8]:

$$\Gamma_e = \frac{1}{4}n_e v_e, \tag{22}$$

where n_e and v_e are the electron density and velocity respectively.

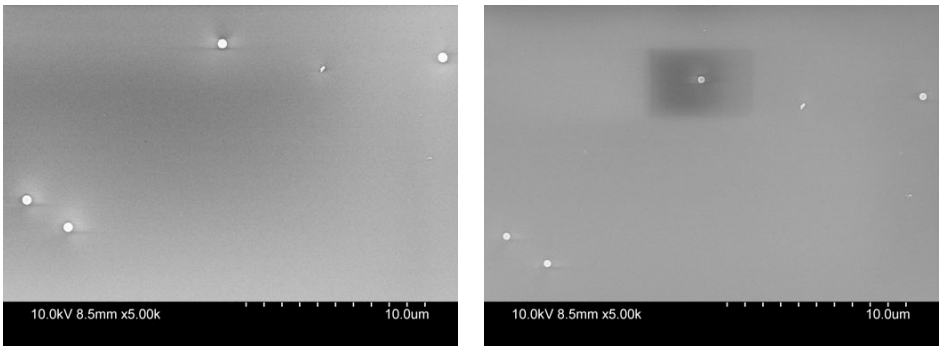

(a) (b)

Fig. 6. The before and after SEM's of the removal experiment for PSL particles on an SiO_2 surface. The sample is processed with a 2 kW He plasma at 10.1 $\pm$ 0.2 mTorr with a +20.1 $\pm$ 0.5 volt bias applied to the sample holder holding the insulating sample. The removal rate calculated after 5 minutes of processing is 8.3x10$^6\pm$ 6.9x10^5 nm^3/min.

3 RESULTS

Numerous experiments have been conducted to show the removal of various contaminants from surfaces. In earlier work, the complete removal of polystyrene latex (PSL) nanoparticles has been shown at a rate of 1.2x10$^7\pm$ 1.3x10^5 nm^3/min [10]. These removal results were shown utilizing the PACMAN technique to clean PSL contaminants from silicon wafers. Also shown in previous work, the cleaning rate of carbon grown by e-beam irradiation of a sample in the presence of dodecane is 3.0x10^6 $\pm$ 1.3x10^5 nm^3/min [10]. Current work has been directed at achieving the cleaning of organic contaminants from insulating substrates, with EUV mask blank cleaning in mind. As shown in Figure 6, when applying the cleaning recipe optimized for a conducting substrate, the cleaning of 500 nm PSL from a wafer with 2 micron of SiO_2 proceeds at a cleaning rate of 8.3x10$^6\pm$ 6.9x10^5 nm^3/min. Further optimization of the PACMAN technique recovers the removal rate observed on the conducting substrate, showing that the PACMAN technique can be used to clean conducting and insulating substrates at the same cleaning rate.

Work has also been completed showing the removal of environmental carbon defects from EUV substrates. Carbon defects were detcted on an EUV mask blank, where the defects were produced by the EUV tool. The defect volumes were measured via AFM pre processing, and the volume was used to calculated a spherically equivalent volume diameter (SEVD). The EUV mask blank was exposed to the PACMAN cleaning process, and subsequent post-processing AFM volume measurement conducted. Refinements of the calculated cleaning rate of these environmental contaminants on an EUV mask blank are still being completed, however, as shown in Figure 7 and Figure 8, the PACMAN technique achieves cleaning of environmental contaminats.

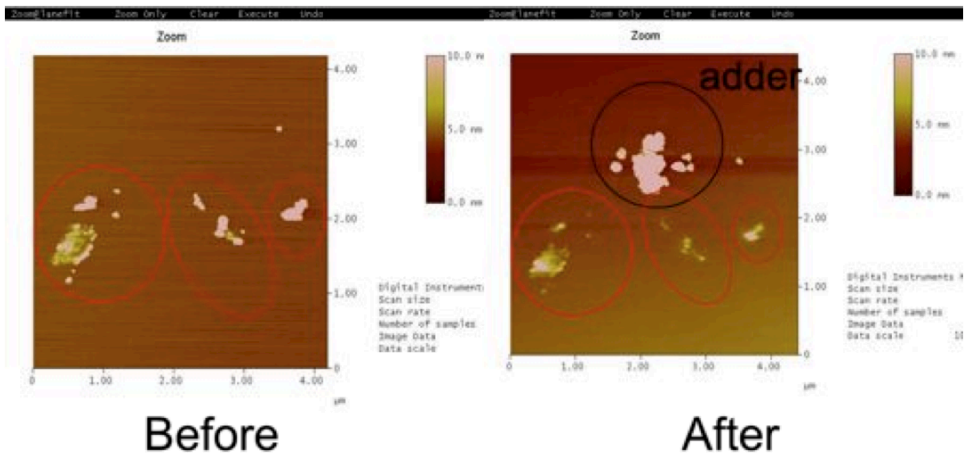

Fig. 7. Shown is the AFM map of environmental carbon contaminants on an EUV mask blank before and after PACMAN cleaning. Cleaning was not carried to complete removal in order to faciliate that calculationg of a cleaning rate.

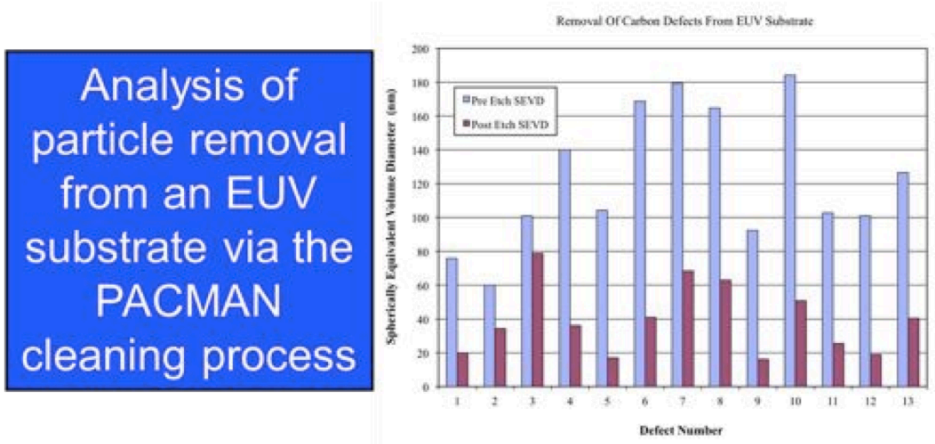

Fig. 8. Shown is the spherical equiavlent volume diameter (SEVD) of defects detected pre and post PACMAN cleaning. As shown, all defects show some removal. The difference in the removal from contaminant to contaminant is attributed to material differences in the contaminant particle.

4 CONCLUSIONS

It has been shown that hydrocarbon contaminants (PSL spheres) can be removed at a rate of $1.2\text{x}10^7 \pm 5.1\text{x}10^5$ nm^3/min from both conduting and insulating surfaces. Carbon contaminants grown via an electron beam irradiation of a surface can be cleaned at a rate of $3.0\text{x}10^6 \pm 1.3\text{x}10^5$ nm^3/min. Also, removal of environmental contaminants from an EUV tool on an insulating EUV blank substrate has been shown. No surface damage either by surface sputtering, layer erosion, or surface roughening has been observed while using the PACMAN cleaning technique. Also, the PACMAN technique has no theoretical size limit for the contaminants that can be cleaned.

Further refinement of the PACMAN technique for cleaning environmental carbon contaminants from lithographic surfaces will be continued in the CPMI as well as the cleaning of other particle types from a variety of surfaces.

The authors would like to thank Sematech for funding, the Micro and Nano Technology Lab at the University of Illinois Urbana-Champaign, as well as undergraduate research assistant Michael McGuire.

References

[1] S. Sasaki, S. Takamura, S. Watanabe, S. Masuzaki, T. Kato, and K. Kadota. Helium I Line Intensity Ratios in a Plasma for the Diagnostics of Fusion Edge Plasmas. *Rev. Sci. Instruments*, 67(10), 1996.

[2] W. Sesselmann, B. Woratschek, J. Kuppers, G. Ertl, and H. Haberland. Interaction of metastable noble-gas atoms with transition-metal surfaces: Resonance ionization and Auger neutralization. *Physical Review B*, 35(4):1547–1559, 1987.

[3] N. Miura and J. Hopwood. Metastable helium density probe for remote plasmas. *Review of Scientific Instruments*, 80:113502, 2009.

[4] A. Bard, KK Berggren, JL Wilbur, JD Gillaspy, SL Rolston, JJ McClelland, WD Phillips, M. Prentiss, and GM Whitesides. Self-assembled monolayers exposed by metastable argon and metastable helium for neutral atom lithography and atomic beam imaging. *Journal of Vacuum Science & Technology B: Microelectronics and Nanometer Structures*, 15:1805, 1997.

[5] M. Kurahashi and Y. Yamauchi. Metastable Helium Atom Stimulated Desorption of H^{+} Ion. *Physical review letters*, 84(20):4725–4728, 2000.

[6] N. Ueno, H. Yasufuku, S. Kera, KK Okudaira, and Y. Harada. Surface Imaging Using Electrons Excited by Metastable-Atom Impacts. *Lecture Notes in PHysics - New York then Berlin*, pages 131–144, 2002.

[7] M. Kurahashi and Y. YAMAUCHI. Observation of H+ desorption stimulated by the impact of metastable helium atoms. *Surface Science*, 454(1-2):300–304, 2000.

[8] D.N. Ruzic. *Electric Probes for Low Temperature Plasmas*. American Vacuum Society, 1994.

[9] M.A. Lieberman and A.J. Lichtenberg. *Principles of Plasma Discharges and Materials Processing*. John Wiley and Sons, Inc., 1994.

[10] WM Lytle, RE Lofgren, V. Surla, MJ Neumann, and DN Ruzic. Removal of carbon and nanoparticles from lithographic materials by plasma assisted cleaning by metastable atom neutralization (PACMAN). In *Proceedings of SPIE*, volume 7636, page 76360O, 2010.